

# Search for three alpha states around an $^{16}\text{O}$ core in $^{28}\text{Si}$

T. Ichikawa,<sup>1</sup> N. Itagaki,<sup>1</sup> Y. Kanada-En'yo,<sup>2</sup> Tz. Kokalova,<sup>3</sup> and W. von Oertzen<sup>4</sup>

<sup>1</sup>*Yukawa Institute for Theoretical Physics, Kyoto University, Kyoto 606-8502, Japan*

<sup>2</sup>*Department of Physics, Kyoto University, Kyoto 606-8502, Japan*

<sup>3</sup>*School of Physics and Astronomy, University of Birmingham, Edgbaston, B15 2TT, Birmingham, UK*

<sup>4</sup>*Helmholtz-Zentrum Berlin, Hahn-Meitner-Platz 1, 14109 Berlin, Germany*

(Dated: November 20, 2018)

We investigate the existence of weakly coupled gas-like states comprised of three  $\alpha$  particles around an  $^{16}\text{O}$  core in  $^{28}\text{Si}$ . We calculate the excited states in  $^{28}\text{Si}$  using the multi-configuration mixing method based on the  $^{16}\text{O} + 3\alpha$  cluster model. We also include the  $^{16}\text{O} + ^{12}\text{C}$  and  $^{24}\text{Mg} + \alpha$  basis wave functions prepared by the generator coordinate method. To identify the gas-like states, we calculate the isoscalar monopole transition strengths and the overlap of the obtained states with the geometrical cluster wave function and the Tohsaki-Horiuchi-Schuck-Röpke (THSR) wave function. The results show that the obtained fourth and twelfth states significantly overlap with the THSR wave function. These two states clearly coexist with the  $^{16}\text{O} + ^{12}\text{C}$  cluster states, emerging at similar energies. The calculated isoscalar monopole strengths between those two states are significantly large, indicating that the states are members of the excitation mode. Furthermore, the calculated root-mean-squared (RMS) radii for these states also suggest that a layer of gas-like three  $\alpha$  particles could exist around the surface of the  $^{16}\text{O}$  core, which can be described as a “two-dimensional gas” in the intermediate state before the Hoyle-like three  $\alpha$  states emerge.

PACS numbers: 21.10.-k, 21.60.-n, 21.60.Gx, 27.20.+n, 27.30.+t

The investigations of excited states in light-mass nuclei provide a good opportunity to study the rich variety of nuclear structures of quantum many-body systems. One of these states is the well known Hoyle state in  $^{12}\text{C}^*$  [1]. The Hoyle state is the second  $0^+$  state in  $^{12}\text{C}^*$ , with an excitation energy of 7.65 MeV, just above the  $3\alpha$  decay threshold energy. Many theoretical attempts have been performed to reproduce its energy and geometrical properties. It was found, that it is difficult to reproduce those values by calculations based only on the shell model. On the other hand, the microscopic three  $\alpha$  cluster models successfully describe the properties of the Hoyle state (such as the observed  $\alpha$ -decay width) and indicate that the three  $\alpha$  state develops well in the  $0_2^+$  state [2, 3].

Recent calculations, using the  $\alpha$  cluster model suggest that in the Hoyle state, the three “gas-like”  $\alpha$  particles are weakly coupled with each other at near the three  $\alpha$ -decay threshold energy [4, 5]. Based on this picture, the Tohsaki-Horiuchi-Schuck-Röpke (THSR) wave function was proposed. This wave function describes the  $\alpha$  particles as independent, with their center-of-mass motion, in the same  $0S$  state of the harmonic oscillator, having a large oscillator parameter. Using this wave function, Tohsaki *et al.* proposed the extremely large RMS nuclear radius for the  $0_2^+$  state in  $^{12}\text{C}$  [4].

Those studies have triggered interest in whether such gas-like states exist in heavier-mass nuclei. Funaki *et al.* searched for gas-like four  $\alpha$  states in  $^{16}\text{O}^*$  using the microscopic  $\alpha$  cluster model coupled with the THSR wave function [6, 7]. In this connection, the existence of weakly coupled gas-like  $\alpha$  cluster states around a core has been recently suggested [8–12]. To study this, the Monte-Carlo technique for the THSR wave function was proposed [13]. The possibility of a gas-like three  $\alpha$  cluster state around  $^{40}\text{Ca}$  in  $^{52}\text{Fe}$  has been discussed using this technique [14]. To identify such gas-like states experimentally, the measurement of an isoscalar monopole transition strength has been proposed [15, 16]. The enhancement of

the transition strength would correspond to the development of such cluster structure. In this respect, gas-like two  $\alpha$  states around an  $^{16}\text{O}$  core in  $^{24}\text{Mg}$  have been investigated both theoretically [15, 17–19] and experimentally [16, 20, 21].

The aim of the present paper is to search for the weakly coupled gas-like three  $\alpha$  cluster states around an  $^{16}\text{O}$  core in  $^{28}\text{Si}$ . In analogy to the three  $\alpha$ -particle Hoyle state in  $^{12}\text{C}$ , the existence of states, similar to the Hoyle state with three  $\alpha$ -particles around an  $^{16}\text{O}$  core can be expected. However, in  $^{28}\text{Si}$ , many strongly coupled cluster states would emerge at and below/above the ( $^{16}\text{O} + 3\alpha$ ) decay threshold energy [22–24]. Three  $\alpha$  particles around an  $^{16}\text{O}$  core would form the strongly coupled  $^{12}\text{C}$  state, to gain the inter cluster potential energy. An important feature is that these weakly and strongly coupled systems would coexist and that their emergences compete with each other. To discuss the existence of the weakly coupled gas-like three  $\alpha$  state around an  $^{16}\text{O}$  core, it is important to completely understand the occurrence of all strongly coupled cluster states within the orthogonality condition among the states.

To investigate the existence of the gas-like three  $\alpha$  state around the  $^{16}\text{O}$  core, we calculate the excited states of  $^{28}\text{Si}$  using the  $^{16}\text{O} + 3\alpha$  cluster model. We superpose many randomly generated Slater determinants, which correspond to the multi-configuration mixing (MCM) method. To describe the molecular states, we also include the basis wave functions with  $^{16}\text{O} + ^{12}\text{C}$  and  $^{24}\text{Mg} + \alpha$  configurations prepared by the generator coordinate method (GCM). In the MCM calculations, it becomes often difficult to identify the structure of the obtained results as the number of the basis wave functions increases, because many states couple with each other. Thus, we must develop the analyzing method for the results from the full large scale calculations. To identify the relevant states, we calculate the overlap of the obtained results with the THSR and the geometrical cluster wave functions. We also calculate the

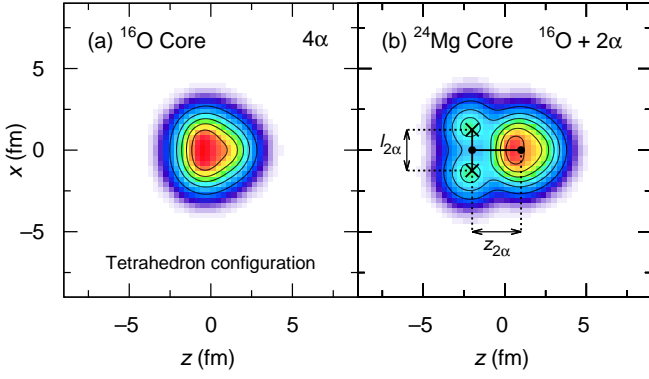


FIG. 1. (Color online) Density plots of the basis wave functions for the  $^{16}\text{O}$  and  $^{24}\text{Mg}$  cores. The contours correspond to multiple steps of  $0.2 \text{ fm}^{-2}$ . The color is normalized by the largest density in each plot.

RMS radius and the isoscalar monopole transition strength. We show below how the gas-like three  $\alpha$  states emerge and how they connect with the ground state.

In the present study, we use Brink's  $\alpha$ -cluster model [25]. In this approach the wave function for  $^{28}\text{Si}$  is described by the Slater determinant of the seven  $\alpha$  clusters. The wave function of the  $\alpha$  cluster,  $\phi_\alpha$ , is described by the direct product of four wave functions for each nucleon (proton and neutron with spin down and up). The spacial part of the wave function for the  $\alpha$  cluster is given by  $\phi_\alpha(\vec{R}) \propto \prod_{i=1}^4 \exp[-\nu(\vec{r}_i - \vec{R})^2]$ , where  $\vec{R}$  denotes the center position vector of the Gaussian function,  $\vec{r}_i$  denotes the spatial coordinate of each nucleon, and  $\nu$  denotes the size parameter. We take  $\nu = 1/2b^2$  with  $b = 1.46 \text{ fm}$  in the calculations. To describe the  $\alpha$  cluster, we take the same  $\vec{R}$  for all four nucleons.

To calculate the excited states, we superimpose many basis wave functions described by the Brink  $\alpha$ -cluster model for  $^{28}\text{Si}$ . In this study, we prepare the basis wave functions using  $^{16}\text{O} + 3\alpha$  cluster configurations to investigate the three  $\alpha$  states around the  $^{16}\text{O}$  core. To take into account the molecular states, we also prepare the basis wave functions using  $^{16}\text{O} + ^{12}\text{C}$  and  $^{24}\text{Mg} + \alpha$  configurations based on the GCM.

We first prepare the cluster wave functions using the  $^{16}\text{O}$ ,  $^{12}\text{C}$ , and  $^{24}\text{Mg}$  configurations. The cluster wave functions of  $^{16}\text{O}$ ,  $^{12}\text{C}$ , and  $^{24}\text{Mg}$  with the center-of-mass position  $\vec{R}$  are denoted by  $\Phi_{^{16}\text{O}}(\vec{R})$ ,  $\Phi_{^{12}\text{C}}(\vec{R})$ , and  $\Phi_{^{24}\text{Mg}}(\vec{R})$ , respectively. For  $\Phi_{^{16}\text{O}}(\vec{R})$ , we take a tetrahedron configuration with four  $\alpha$  clusters. The additional three  $\alpha$ 's form a triangle, it is perpendicular to the  $z$ -axis and one side of the triangle is parallel to the  $x$ - $z$  plane. The further residual  $\alpha$  particle is placed on the positive  $z$  direction. Figure 1(a) shows the total density of  $\Phi_{^{16}\text{O}}$  used in this study. The  $\alpha$ - $\alpha$  distance between each center position of the Gaussian functions of the four  $\alpha$ 's in the  $^{16}\text{O}$  core is quite small,  $0.5 \text{ fm}$ , in order to simulate the doubly closed configuration of the shell model.

For  $\Phi_{^{12}\text{C}}(\vec{R})$ , we take the equilateral triangle configuration of the three  $\alpha$  clusters with a length of  $a \text{ fm}$ . The triangle is placed on the  $x$ - $z$  plane and a side (two of the  $\alpha$  clusters) is perpendicular to the  $z$  axis in the center-of-mass frame of

$^{12}\text{C}$ . The residual  $\alpha$  cluster is placed on the negative  $z$  axis. We also take three different configurations by rotating the  $\alpha$ -cluster triangle on the  $x$  axis with angles of  $0^\circ$ ,  $45^\circ$ , and  $90^\circ$ . Those configurations are denoted by  $^{12}\text{C}_{\parallel}$ ,  $^{12}\text{C}_{\perp}$  and  $^{12}\text{C}_{\perp}$ .

The wave function of  $\Phi_{^{24}\text{Mg}}(\vec{R})$  is an isosceles configuration with  $\Phi_{^{16}\text{O}}(\vec{R}_0)$  and two  $\alpha$  clusters. Figure 1(b) shows the density plot of  $\Phi_{^{24}\text{Mg}}$  used in this study. The configuration of  $\Phi_{^{16}\text{O}}(\vec{R}_0)$  is the same as mentioned above. The isosceles triangle is placed on the  $x$ - $z$  plane and the base of the two alpha clusters is perpendicular to the  $z$  axis. The crosses denote the positions of the two  $\alpha$  clusters. The distance between the two  $\alpha$  clusters is denoted by  $l_{2\alpha}$ . The distance between  $\Phi_{^{16}\text{O}}(\vec{R}_0)$  and the  $z$  position of the base is denoted by  $z_{2\alpha}$ . We determine  $l_{2\alpha}$  and  $z_{2\alpha}$  by minimizing the expectation value of the total energy for  $\Phi_{^{24}\text{Mg}}$ . We here take  $l_{2\alpha} = 2.5 \text{ fm}$  and  $z_{2\alpha} = 3.0 \text{ fm}$ .

We next prepare the basis wave functions using  $^{16}\text{O} + 3\alpha$ ,  $^{16}\text{O} + ^{12}\text{C}$ , and  $^{24}\text{Mg} + \alpha$  cluster configurations. The basis wave function using the  $^{16}\text{O} + 3\alpha$  cluster configuration,  $\Psi_{^{16}\text{O}+3\alpha}^{(i)}$ , is given by  $\Psi_{^{16}\text{O}+3\alpha}^{(i)} = [\mathcal{A}\Phi_{^{16}\text{O}}(\vec{R}_0)\phi_\alpha(\vec{R}_1)\phi_\alpha(\vec{R}_2)\phi_\alpha(\vec{R}_3)]_i$ , where  $\mathcal{A}$  denotes the antisymmetrization operator. We first take  $\vec{R}_0 = 0$  and the positions of the three  $\alpha$  clusters  $\vec{R}_1$ ,  $\vec{R}_2$ , and  $\vec{R}_3$  are randomly generated under the condition of the distributed probability  $w(\vec{R}_i)$ . In this study, we use  $w(\vec{R}_i) \propto \exp[-\vec{R}_i^2/\sigma^2]$ , where  $\sigma$  is the size parameter. Subsequently, the center-of-mass correction for  $\Psi_{^{16}\text{O}+3\alpha}^{(i)}$  was performed.

The basis wave functions using the  $^{16}\text{O} + ^{12}\text{C}$  configuration,  $\Psi_{^{16}\text{O}+^{12}\text{C}}^{(i)}$ , is given by  $\Psi_{^{16}\text{O}+^{12}\text{C}}^{(i)} = [\mathcal{A}\Phi_{^{16}\text{O}}(\vec{R}_0)\Phi_{^{12}\text{C}}(\vec{R})]_i$ . The  $^{12}\text{C}$  cluster is shifted to the positive  $z$  direction. Here, the distance between the center-of-mass positions of the  $^{16}\text{O}$  and  $^{12}\text{C}$  clusters is denoted by  $d_{^{16}\text{O},^{12}\text{C}}$ . The basis wave functions using  $^{24}\text{Mg} + \alpha$  configurations,  $\Psi_{^{24}\text{Mg}+\alpha}^{(i)}$ , is given by  $\Psi_{^{24}\text{Mg}+\alpha}^{(i)} = [\mathcal{A}\Phi_{^{24}\text{Mg}}(\vec{R}_0)\phi_\alpha(\vec{R})]_i$ . The wave function of  $\phi_\alpha(\vec{R})$  is placed on the  $x$ ,  $y$ , or  $z$  axes. Those configurations are denoted by  $^{24}\text{Mg} + \alpha_x$ ,  $^{24}\text{Mg} + \alpha_y$ , and  $^{24}\text{Mg} + \alpha_z$ . The distance between the center-of-mass positions of the  $^{24}\text{Mg}$  and  $\alpha$  clusters is denoted by  $d_{^{24}\text{Mg}-\alpha}$ .

In the calculation, we generate 1000 wave functions for  $\Psi_{^{16}\text{O}+3\alpha}^{(i)}$ . For  $\Psi_{^{16}\text{O}+^{12}\text{C}}^{(i)}$ , we take four and eight values for  $a$  and  $d_{^{16}\text{O},^{12}\text{C}}$  in each angle of  $^{12}\text{C}_{\parallel}$ ,  $^{12}\text{C}_{\perp}$  and  $^{12}\text{C}_{\perp}$ , respectively. Those correspond to  $a = (1.0, 2.0, 3.0, 4.0) \text{ fm}$  and  $d_{^{16}\text{O},^{12}\text{C}} = (1.0, 2.0, \dots, 8.0) \text{ fm}$ . For  $\Psi_{^{24}\text{Mg}+\alpha}^{(i)}$ , we take eight values for  $d_{^{24}\text{Mg}-\alpha}$  corresponding to  $d_{^{24}\text{Mg}-\alpha} = (1.0, 2.0, \dots, 8.0) \text{ fm}$  in each direction of  $\alpha_x$ ,  $\alpha_y$ , and  $\alpha_z$ .

Thus, the total number of the basis wave functions is 1120. The total wave function  $\Psi_{\text{Total}}$  is described with the linear combination of the basis wave functions given by  $\Psi_{\text{Total}} = \sum_i c_i P^+ P_{00}^0 \Psi^{(i)}$ , where  $\Psi^{(i)}$  denotes each basis wave function. The coefficient  $c_i$  is determined by diagonalizing the total Hamiltonian. The symbols  $P^+$  and  $P_{00}^0$  denote the projection operator for the parity and angular-momentum ( $J = M = K = 0$ ) to the  $0^+$  state, respectively. We here only calculate the  $0^+$  states to focus on the gas-like three  $\alpha$  state. We perform the center-of-mass correction and the parity and angular momentum projections to the  $0^+$  state for each basis wave function

numerically. For the calculations of the angular-momentum projection,  $24 \times 32 \times 24$  grids points are taken with respect to the  $\alpha$ ,  $\beta$ , and  $\gamma$  directions of the Euler angle. For the total Hamiltonian, we use the Volkov No.2 effective  $N$ - $N$  interaction [26]. In the calculation, the Majorana exchange parameter,  $M$ , is chosen to be 0.645 so as to reproduce the binding energy of  $^{28}\text{Si}$ . In the calculation, the cluster decay threshold energies for  $^{16}\text{O} + 3\alpha$  and  $^{16}\text{O} + ^{12}\text{C}$  are  $-189.29$  MeV and  $-186.48$ , respectively.

To identify the gas-like  $\alpha$  states, we calculate the overlap between the obtained states and the THSR wave function. The THSR wave function with the gas-like three  $\alpha$  particles around an  $^{16}\text{O}$  core,  $\Psi_{\text{THSR}}^{(\sigma)}$ , is given by

$$\begin{aligned} \Psi_{\text{THSR}}^{(\sigma)} &= \int d\vec{R}_1 d\vec{R}_2 d\vec{R}_3 \cdot \exp[-(\vec{R}_1^2 + \vec{R}_2^2 + \vec{R}_3^2)/\sigma^2] \\ &\quad \cdot [\mathcal{A}\phi_{^{16}\text{O}}(\vec{R}_0)\phi_\alpha(\vec{R}_1)\phi_\alpha(\vec{R}_2)\phi_\alpha(\vec{R}_3)] \\ &= \mathcal{A}\phi_{^{16}\text{O}}(\vec{R}_0) \prod_{i=1}^3 \int d\vec{R}_i \phi_\alpha(\vec{R}_i) \exp[-\vec{R}_i^2/\sigma^2], \quad (1) \end{aligned}$$

where  $\sigma$  is the size parameter of the gas-like  $\alpha$  state. We can perform the Monte-Carlo integration for Eq. 1, when the exponential term  $\exp[-\vec{R}_i^2/\sigma^2]$  in Eq. 1 is regarded as the weight factor of the randomly generated integral points. We also perform the parity and angular-momentum projections to the  $0^+$  state at each generated integral point. Then, the Monte-Carlo THSR wave function  $\Psi_{\text{THSR}}^{(\sigma)}$  is given by  $\Psi_{\text{THSR}}^{(\sigma)} = \sum_i P^+ P_{00}^0 \Psi_{^{16}\text{O}+3\alpha}^{(i)}$ . The integral points for  $\vec{R}_1$ ,  $\vec{R}_2$ , and  $\vec{R}_3$  are randomly generated under the condition of the weight factor  $w(\vec{R}_i)$  given by  $w(\vec{R}_i) \propto \exp[-\vec{R}_i^2/\sigma^2]$ . In this study, we calculate the THSR wave function with  $\sigma = 3, 4$  and  $5$  fm. For the Monte-Carlo calculations, we use 900 randomly generated basis wave functions for each  $\sigma$ . The expectation values of the total energy for those with  $\sigma = 3, 4$  and  $5$  converge well at energies of  $-191.39, -188.48$  and  $-182.33$  MeV, respectively.

To investigate the properties of the states obtained in this procedure, we also calculate the isoscalar monopole-transition strength and the RMS radius. Here, the unit of the transition strength,  $B_0(\text{IS0})$ , is taken as the value obtained from the  $1s$  to the  $2s$  states, described by the single-particle wave function of the three-dimensional harmonic oscillator. The value of  $B_0(\text{IS0})$  is then given by  $B_0(\text{IS0}) = \sqrt{5}b^2 \text{ fm}^2$  [15]. In the present study, we take  $B_0(\text{IS0}) = 4.77 \text{ fm}^2$  with  $b = 1.46$ .

Figure 2 (a) shows the convergence behavior of the states measured from the  $^{16}\text{O} + 3\alpha$  decay threshold energy versus the number of the basis wave functions. We plot here only the results below the 15th state. In Fig. 2(a), the gray area (i) denotes the results calculated with the subspace for the  $^{16}\text{O} + ^{12}\text{C}_\perp$ ,  $^{12}\text{C}_\parallel$ , and  $^{12}\text{C}_z$  configurations. The gray area (ii) also denotes those for the  $^{24}\text{Mg} + \alpha_x, \alpha_y$ , and  $\alpha_z$  configurations in addition to the  $^{16}\text{O} + ^{12}\text{C}$  components. The lowest energy in the calculated states with the total wave functions is  $-24.64$  MeV, which is in good agreement with the experimental value of  $-24.03$  MeV.

We first investigate the structure of the ground (first) state. This state corresponds to the prolate shape with a significant

$^{16}\text{O} + ^{12}\text{C}_\perp$  cluster component, which originates from the lowest state of the results of the gray area (i) in Fig. 2(a). The RMS radius obtained for this state is 2.80 fm. To clarify the cluster structure, the overlap of the obtained states with the wave functions using  $^{16}\text{O} + ^{12}\text{C}$  and  $^{24}\text{Mg} + \alpha$  configuration is calculated. Figure 3 shows the density plots of the wave functions maximally overlapping with the calculated states. The lowest state overlaps maximally with the  $^{16}\text{O} + ^{12}\text{C}_\perp$  configuration of 78.5% at  $a = 2.0$  fm and  $d_{^{16}\text{O},^{12}\text{C}} = 3.0$  fm (see Fig. 3(a)).

The second state corresponds to the one-body oblate shape. The obtained RMS radius is 2.77 fm, which is somewhat smaller than that of the first state. The second state overlaps maximally with the  $^{16}\text{O} + ^{12}\text{C}_\parallel$  configuration of 17.3% at  $a = 3.0$  fm and  $d_{^{16}\text{O},^{12}\text{C}} = 1.0$  fm, but many other components also have similar overlaps at small  $d_{^{16}\text{O},^{12}\text{C}}$ . Thus, this state is the compact one-body system rather than a specific cluster state. In Brink's  $\alpha$ -cluster model without the spin-orbit force, the shape configurations for the first and second  $0^+$  states are prolate and oblate (pentagon), respectively. This shows that the results of our calculations are consistent with previous studies, although the experimental data suggest that the ground and the third  $0^+$  states correspond to the oblate and the prolate shapes, respectively [27].

We next investigate the structure of the excited states. Figure 2(b) and (c) show the calculated isoscalar monopole-transition strength from the first and second states in the unit of  $B_0(\text{IS0})$ , respectively. Figure 2(d), (e), and (f) show the calculated overlaps between the obtained states and the THSR wave function with  $\sigma = 3, 4$ , and  $5$  fm, respectively. Below, we only discuss the characteristic results which can be identified by the analysis.

In Figure 2 (d), (e), and (f), we can see that the fourth and twelfth states significantly overlap with the THSR wave function. These states are candidates for the gas-like three  $\alpha$  state discussed in this study. The overlap between the fourth state and the THSR wave functions with  $\sigma = 3, 4$ , and  $5$  fm are 16.7%, 9.8% and 3.3%, respectively. Those overlaps for the twelfth state are 20.0%, 13.7% and 4.9%. We also orthogonalize the THSR wave functions with  $\sigma = 3, 4$ , and  $5$  fm and calculate the overlaps, but the results are very similar to the largest value with the single THSR wave function. The RMS radii obtained for the fourth and the twelfth states are 2.92 and 3.02 fm, respectively. These values are somewhat spatially extended rather than that of the first and second states.

In addition, we obtain remarkably strong transition strength from the fourth to twelfth states by  $B(\text{IS0})/B_0(\text{IS0}) = 3.20$ , indicating that those states strongly correlate with each other due to the cluster excitation. We thus consider that the fourth and twelfth states are a member of the new excitation mode. We also obtain a relatively large transition strength from the first to the fourth states by  $B(\text{IS0})/B_0(\text{IS0}) = 2.21$  (see Fig. 2 (b)), suggesting that this new excitation mode is built on the first state with the prolate shape.

The sixth state has the strongest transition strength from the ground state by  $B(\text{IS0})/B_0(\text{IS0}) = 3.67$ . This state overlaps maximally with the  $^{16}\text{O} + ^{12}\text{C}_\perp$  configuration of 42.2% at  $a = 2.0$  fm and  $d_{^{16}\text{O},^{12}\text{C}} = 4.0$  fm (see Fig. 3(b)). The ob-

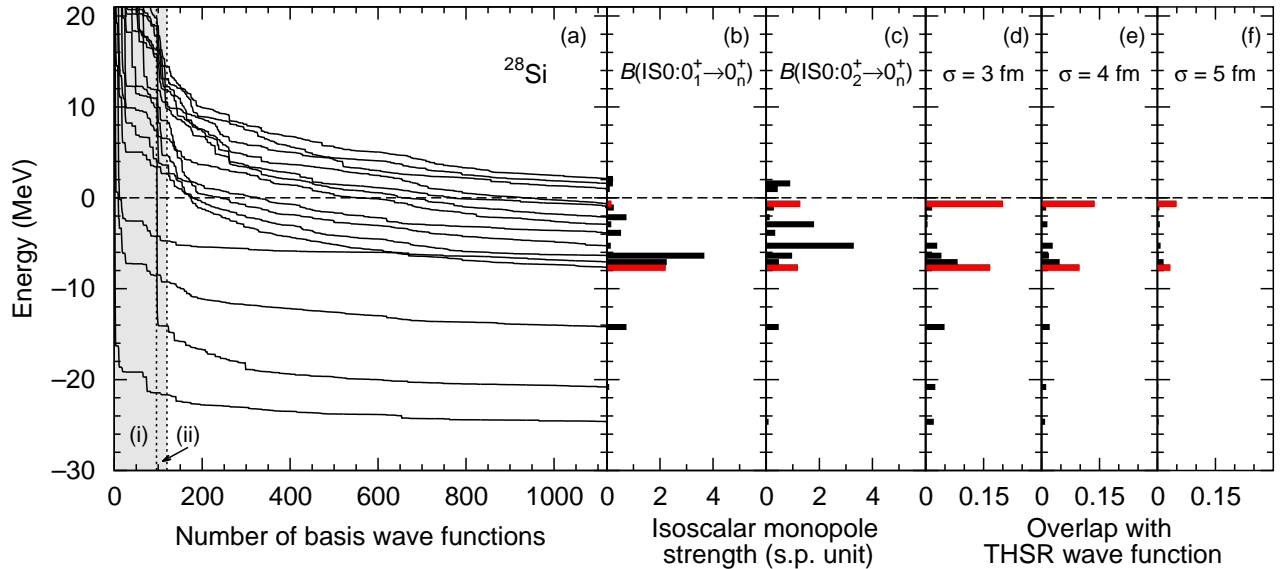


FIG. 2. (Color online) (a) Convergence behavior of the calculated energies versus the number of basis wave functions measured from the  $^{16}\text{O} + 3\alpha$  decay threshold energy. In the gray area denoted by (i) and (ii), we use the basis wave functions with  $^{16}\text{O} + ^{12}\text{C}$  and  $^{24}\text{Mg} + \alpha$  configurations, respectively. (b) and (c) Isoscalar monopole-transition strength from the first and second states in the unit of the single-particle (S.P.) excitation from the  $1s$  to the  $2s$  states, respectively. (d), (e), and (f) Overlap between each state and the THSR wave function with  $\sigma = 3, 4,$  and  $5$  fm, respectively.

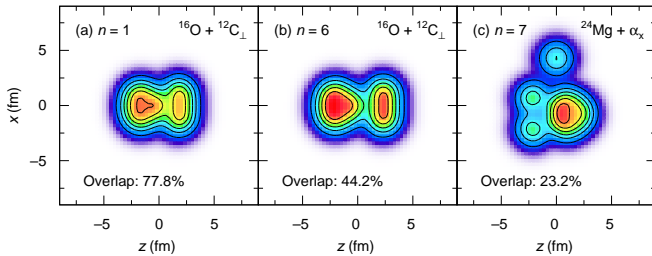


FIG. 3. (Color online) Density plots of the basis wave function overlapping maximally with the calculated states. The contours correspond to multiples of  $0.2 \text{ fm}^{-2}$ . The color is normalized by the largest density in each plot.

tained RMS radius is  $2.95$  fm. This corresponds to the  $^{16}\text{O} + ^{12}\text{C}$  molecular state where the relative motion between two clusters is excited from the ground (first) to the higher-nodal states. The seventh state also has strong transition strength from the second state by  $B(\text{IS}0)/B_0(\text{IS}0) = 3.30$ . This state is the cluster excitation of the  $^{24}\text{Mg} + \alpha_x$  configuration. The maximum overlap between the seventh state and the  $^{24}\text{Mg} + \alpha_x$  configuration is  $23.2\%$  at  $d_{24\text{Mg}-\alpha} = 5.0$  fm (see Fig. 3(c)). The obtained RMS radius is  $2.93$  fm.

An important observation is that the fourth and the twelfth states do not largely overlap with any geometrical configurations of the  $\alpha$  clusters. Despite this, the RMS radii for these states are considerably extended to similar extent as other cluster states. The fourth and twelfth excited states significantly overlap with the THSR wave function not only with  $\sigma = 3$  fm but also  $\sigma = 4$  fm. This suggests the existence of gas-like three  $\alpha$  particles spreading to the out-

side of the  $^{16}\text{O}$  core. To see the extent of the spreading for the gas-like three  $\alpha$  particles, we estimate the RMS radius of the three  $\alpha$  particles. Here, the effect of the  $^{16}\text{O}$  core is subtracted by neglecting the recoil correction. The RMS radius for the three  $\alpha$  particles,  $r_{\text{RMS}}^{(3\alpha)}$ , is then given by  $r_{\text{RMS}}^{(3\alpha)} = \sqrt{(28 \langle r^2(^{28}\text{Si}) \rangle - 16 \langle r^2(^{16}\text{O}) \rangle) / 12}$ , where  $\langle r^2(^{28}\text{Si}) \rangle$  and  $\langle r^2(^{16}\text{O}) \rangle$  denote the expectation value of the squared radius for the  $^{28}\text{Si}$  and the  $^{16}\text{O}$  core, respectively. We calculate  $\langle r^2(^{28}\text{Si}) \rangle$  without the center-of-mass correction. We also obtain  $\sqrt{\langle r^2(^{16}\text{O}) \rangle} = 2.2$  fm with the tetrahedron configuration of four  $\alpha$ 's. The calculated RMS radii of the three  $\alpha$  particles for the first, fourth, and twelfth states are  $3.45, 3.67,$  and  $3.86$  fm, respectively. Those are indeed expanded with increasing excitation energies. However, the spatial distributions for those three  $\alpha$  particles are not so widely spread rather than that of the Hoyle state in  $^{12}\text{C}$  because of the existence of the attractive  $^{16}\text{O}$  core.

Therefore, we consider that the fourth and twelfth states are members of a new type of excitation mode built on the prolate state, which has not yet been well established in experiments. In the first excited state of this mode (fourth state), the weakly coupled gas-like three  $\alpha$  particles, without the angular correlations, emerge around the surface of the  $^{16}\text{O}$  core. That can be described as a layer of dilute density formed around a core, which would be regarded as a “two-dimensional (2D) gas”. The emergence of this weakly coupled 2D gas-like state significantly competes with that of the  $^{16}\text{O} + ^{12}\text{C}$  molecular state (sixth state), which have strongly coupled three  $\alpha$ 's of  $^{12}\text{C}$ , as their energies are almost comparable to each other. This indicates, that the energy necessary for the excitation from the strongly coupled  $^{12}\text{C}$  to the weakly coupled three  $\alpha$ 's around the  $^{16}\text{O}$  core is comparable to the relative motion between  $^{16}\text{O}$

and  $^{12}\text{C}$ . Despite this competition, the coexistence of the 2D gas-like and the strongly coupled states is highly possible, as shown in this study.

In the second excited state of this new mode (twelfth state), the gas-like layer is well developed and more spatially expanded, because the isoscalar monopole strength only from the first excited (fourth) state is extremely large. In more highly excited states, the Hoyle-like weakly coupled  $3\alpha$  state, that is a “three-dimensional (3D) gas-like” state around the  $^{16}\text{O}$  core may emerge. Then, the second excited 2D gas-like state would be the intermediate state before the 3D gas-like state emerges and would be directly connected to the 3D gas-like state by the large isoscalar monopole transition strength. However, it is difficult to identify such 3D gas-like states in the present calculations, because many continuum states are coupled with other states in the high excitation energies. The development of analyses, such as the complex scaling and the pseudo-potential method, is necessary when searching for such states.

In summary, we have investigated the existence of weakly coupled gas-like three  $\alpha$  states around an  $^{16}\text{O}$  core. To study this, we have calculated the excited states of  $^{28}\text{Si}$  using the multi-configuration mixing method with the basis wave functions randomly generated by the  $^{16}\text{O} + 3\alpha$  cluster model. We have also included the  $^{16}\text{O} + ^{12}\text{C}$  and  $^{24}\text{Mg} + \alpha$  basis wave functions, prepared by the GCM method to describe well the molecular states. To identify the states, which we have obtained, we have calculated their overlap with the geometrical cluster wave functions and the THSR wave function. Furthermore we have also calculated the RMS radius and the isoscalar monopole transition strength for the obtained states.

We have found that the fourth and twelfth excited states largely overlap with the THSR wave function with  $\sigma = 3$  and 4 fm. The calculated isoscalar monopole strengths are also significantly large from the first to the fourth and from the fourth to the twelfth states, indicating those may be members of a new excitation mode. At around the energy of the fourth excited state, the  $^{16}\text{O} + ^{12}\text{C}$  cluster state, which has three strongly coupled  $\alpha$ 's of  $^{12}\text{C}$ , also emerges, but the fourth state coexists with this state. The calculated RMS radii for the fourth and twelfth states suggests that a layer of dilute three  $\alpha$  particles may exist around the  $^{16}\text{O}$  core. This gas-like structure in the layer would be the intermediate state, before the complete 3D Hoyle-like gas state emerges.

## ACKNOWLEDGMENTS

A part of this research has been funded by MEXT HPCI STRATEGIC PROGRAM. TzK is grateful to the Daphne Jackson trust and STFC for their support. Numerical computation in this work has been carried out at the Yukawa Institute Computer Facility using the SR16000 system. This work was performed as part of the Yukawa International Project for Quark-Hadron Sciences (YIPQS). It was also supported by a Grant-in-Aid for the Global COE Program “The Next Generation of Physics, Spun from Universality and Emergence” from the Ministry of Education, Culture, Sports, Science and Technology (MEXT) of Japan and a Grant-in-Aid for Scientific Research from the Japan Society for the Promotion of Science.

- 
- [1] F. Hoyle, *Astrophys. J. Suppl.* **1**, 121 (1954).  
 [2] E. Uegaki *et al.*, *Prog. Theor. Phys.* **57**, 1262 (1977); *Prog. Theor. Phys.* **59**, 1031 (1978); *Prog. Theor. Phys.* **62**, 1621 (1979).  
 [3] M. Kamimura, *Nucl. Phys.* **A351**, 456 (1981).  
 [4] A. Tohsaki, H. Horiuchi, P. Schuck, and G. Röpke, *Phys. Rev. Lett.* **87**, 192501 (2001).  
 [5] P. Schuck, Y. Funaki, H. Horiuchi, G. Röpke, A. Tohsaki and T. Yamada, *Nucl. Phys.* **A738**, 94 (2004).  
 [6] Y. Funaki, A. Tohsaki, H. Horiuchi, P. Schuck, and G. Röpke, *Phys. Rev. C* **67**, 051306(R) (2003).  
 [7] Y. Funaki, *et al.*, *Mod. Phys. Lett. A* **21**, 2331 (2006); *Phys. Rev. C* **80**, 064326 (2009).  
 [8] Tz. Kokalova *et al.*, *Eur. Phys. J. A* **23**, 19 (2005).  
 [9] Tz. Kokalova, N. Itagaki, W. von Oertzen, and C. Wheldon, *Phys. Rev. Lett.* **96**, 192502 (2006).  
 [10] W. von Oertzen, *Eur. Phys. J. A* **29**, 133 (2006).  
 [11] W. von Oertzen, *Clusters in Nuclei - Vol.1, Lecture Notes in Physics Vol. 818*, edited by C. Beck (Springer, Berlin, 2010), Chap. 1. pp. 109.  
 [12] A.A. Ogloblin, S.A. Goncharov, T.L. Belyaeva, and A.S. Demyanova, *Phys. of Atom. Nucl.* **69**, 1149 (2006).  
 [13] N. Itagaki *et al.*, *Phys. Rev. C* **75**, 037303 (2007); *Phys. Rev. C* **77**, 037301 (2008); *Phys. Rev. C* **78**, 017306 (2008); S. Aoyama and N. Itagaki, *Phys. Rev. C* **80**, 021304(R) (2009).  
 [14] N. Itagaki, Tz. Kokalova, and W. von Oertzen, *Phys. Rev. C* **82**, 014312 (2010).  
 [15] T. Yamada *et al.*, *Prog. Theor. Phys.* **120**, 6 (2008).  
 [16] T. Kawabata *et al.*, *Phys. Lett. B* **646**, 6 (2007).  
 [17] T. Ichikawa, N. Itagaki, T. Kawabata, Tz. Kokalova, and W. von Oertzen, *Phys. Rev. C* **83**, 061301(R) (2011).  
 [18] T. Yoshida *et al.*, *Phys. Rev. C* **79**, 034308 (2009); *Phys. Rev. C* **83** 024301 (2011).  
 [19] S. Peru and H. Goutte, *Phys. Rev. C* **77**, 044313 (2008).  
 [20] T. Wakasa *et al.*, *Phys. Lett. B* **653**, 173 (2007).  
 [21] Y. Sasamoto *et al.*, *Mod. Phys. Lett. A* **21**, 2393 (2006).  
 [22] H. Horiuchi, in *Clusters in Nuclei - Vol.1, Lecture Notes in Physics Vol. 818*, edited by C. Beck (Springer, Berlin, 2010), Chap. 2. pp.57-108.  
 [23] Y. Kanada-En'yo and M. Kimura, in *Clusters in Nuclei - Vol.1, Lecture Notes in Physics Vol. 818*, edited by C. Beck (Springer, Berlin, 2010), Chap. 4. pp.109-128.  
 [24] T. Ichikawa, Y. Kanada-En'yo, and P. Möller, *Phys. Rev. C* **83**, 054319 (2011).  
 [25] D. Brink, *Proc. International School of Physics “Enrico Fermi” course 36*, edited by C. Bloch, (Academic Press, 1966), pp.247-277 (1965).  
 [26] A.B. Volkov, *Nucl. Phys.* **74**, 33 (1965).  
 [27] W. Bauhoff, H. Schultheis, and R. Schultheis, *Phys. Rev. C* **26** 1725 (1982).